Journal of Biomolecular NMR **28:** 205–212, 2004.
KLUWER/ESCOM

Improving the accuracy of NMR structures of large proteins using pseudocontact shifts as long-range restraints

Vadim Gaponenko, Siddhartha P. Sarma*, Amanda S. Altieri, David A. Horita**, Jess Li & R. Andrew Byrd***
Structural Biophysics Laboratory, National Cancer Institute, P.O. Box B, Frederick, MD 21702-1201, U.S.A.

Received 19 May 2003; Accepted 2 October 2003

Key words: deuteration, ILV-labeling, NMR structural accuracy, pseudocontact shifts, residual dipolar coupling, STAT4

Abstract

We demonstrate improved accuracy in protein structure determination for large (≥30 kDa), deuterated proteins (e.g. $STAT4_{NT}$) via the combination of pseudocontact shifts for amide and methyl protons with the available NOEs in methyl-protonated proteins. The improved accuracy is cross validated by Q-factors determined from residual dipolar couplings measured as a result of magnetic susceptibility alignment. The paramagnet is introduced via binding to thiol-reactive EDTA, and multiple sites can be serially engineered to obtain data from alternative orientations of the paramagnetic anisotropic susceptibility tensor. The technique is advantageous for systems where the target protein has strong interactions with known alignment media.

Abbreviations: PCS, pseudocontact shift; RDC, residual dipolar coupling; PAS, paramagnetic anisotropic susceptibility; ppb, parts per billion; RMSD, root mean square deviation.

Introduction

With recent advances in biomolecular NMR, structure determination of proteins of increasing size is becoming possible. The use of TROSY-based techniques and deuteration of aliphatic positions significantly increases the size of macromolecules amenable to NMR (Kay and Gardner, 1997; Pervushin et al., 1997). Although these techniques have greatly facilitated assignment of protein backbone resonances (Tugarinov et al., 2002), acquisition of structural restraints still remains problematic. Only a limited number of NOEs can be measured from exchangeable H^N protons in perdeuterated proteins (Venters et al., 1995). Additional NOEs can be observed from the protonated-methyl groups of Val, Leu, and Ile ($C^{\delta 1}$ only) in highly deuterated proteins (ILV-labeled proteins) (Gardner et al., 1997; Kay and Gardner, 1997). The use of residual dipolar couplings (RDCs) (Tjandra and Bax, 1997) as long-range restraints combined with these limited NOE restraints (Mueller et al., 2000) significantly improves structural precision and accuracy, as was demonstrated for the 42 kDa maltose-binding protein (Choy et al., 2001; Mueller et al., 2000). Difficulties associated with these approaches are (1) the requirement for a large number of RDCs (up to five per residue) to gain significant improvement in structural quality, (2) a redundancy of solutions when simultaneously fitting all RDCs during protein folding (as compared to their traditional use in the refinement of a folded structure), and (3) the lack of translational information from RDCs. Improvements can be obtained if data are available from multiple alignment tensors (Ramirez and Bax, 1998). However, reliance on RDCs to supplement NOEs can be hindered in cases where the protein of interest is incompatible with available

*Present address: Molecular Biophysics Unit, Indian Institute of Science, Bangalore Karnataka – 560012, India.
**Present address: Department of Biochemistry, Wake Forest University School of Medicine, Winston-Salem, NC 27157-1016, U.S.A.
***To whom correspondence should be addressed. E-mail: rabyrd@ncifcrf.gov

alignment media (Kay and Gardner, 1997). For small-to-medium sized proteins, the prognosis for *de novo* folding of proteins using only RDCs (Hus et al., 2001) or combinations of RDCs with structure predictions (Rohl and Baker, 2002) has improved; however, it is not clear that such approaches will be successful for large proteins.

Pseudocontact shifts (PCS) (La Mar et al., 1978), possessing *both* distance and angular dependence, have long been recognized as a valuable tool for structure refinement of metal-binding proteins (Bertini et al., 2001; Hus et al., 2000). Recent advances in protein modification techniques allow introduction of anisotropic probes into the structure of nonmetal-binding proteins (Dvoretsky et al., 2002; Gaponenko et al., 2000, 2002; Feeney et al., 2001). Here, we utilize PCSs as a method for providing long-range restraints in non-metal binding, ILV-labeled proteins. Combining these restraints with the limited set of NOEs available from H^N and methyl protons significantly improves the accuracy of the determined structure for large ($\geq$30 kDa) proteins. To achieve this, a paramagnetic probe is introduced by modifying unique cysteine residues with a thiol-reactive chelator allowing measurement of PCSs and RDCs, without the use of any steric aligning media. Furthermore, by selecting different attachment sites via mutagenesis, and measuring RDCs (Tolman et al., 1995) and PCSs corresponding to each site, long-range distance and angular restraints may be readily obtained from several orientations of the paramagnetic anisotropic susceptibility (PAS) tensor. We demonstrate these methods using the N-terminal domain of STAT4 ($STAT4_{NT}$), a homodimeric 29.4 kDa protein (Baden et al., 1998). We will limit this discussion to the calculation of the 123-residue monomer structure, since this is pertinent to the problem of large single polypeptide chain proteins.

Materials and methods

The ^{13}C and ^{1}H methyl group resonances of the diamagnetic protein were assigned using H(C)(CO)NH (Grzesiek et al., 1993; Montelione et al., 1992) and (H)C(CO)NH (Gardner et al., 1996) experiments. NMR spectra were acquired on a Varian Unity Plus 600 MHz spectrometer. ^{1}H, ^{15}N and ^{13}C assignments have been made for $STAT4_{NT}$ and are available at the BMRB (accession 5997). Interproton distances were measured from the following spectra with the given mixing times (τ_{mix}): 4D $^{15}N/^{15}N$ HSQC-NOESY-HSQC (500 ms); 4D $^{13}C/^{15}N$ HMQC-NOESY-HSQC (175 ms), 4D $^{13}C/^{13}C$ HMQC-NOESY-HSQC (150 ms), and 3D $^{13}C/^{13}C$ methyl-methyl HSQC-NOESY-HSQC (145 ms). The processing and analysis of all NMR data were done using NMRPipe (Delaglio et al., 1995) and ANSIG 3.3 (Kraulis et al., 1989, 1994). Assignment of the resonances from diamagnetic mutant proteins, K92C and T50C, correlate directly with the wild-type protein assignments, and pseudocontact shifted H^N resonances for wt-ILV-$STAT4_{NT}$ were assigned previously (Gaponenko et al., 2002). PCSs for H^N resonances in the K92C and T50C proteins were measured at 800 MHz on a Varian Inova spectrometer. The assignment of shifted methyl protons was made via comparison of the predicted PCS to the observed PCS, based on a preliminary, low-resolution, NOE-based NMR structure (Allegrozzi et al., 2000). In the absence of a preliminary structure, assignment could be made via the standard double or triple resonance correlation experiments used for the diamagnetic ILV-methyl groups combined with the principles used to assign the H^N PCSs (*vide supra*).

Following PCS assignment, the measured values were used for structure calculations. The PCSs can be expressed in a similar manner to dipolar couplings (Gaponenko et al., 2002) as shown by Equation 1:

$$\Delta\delta_{pc} = \frac{P_{ax}}{r^3}(3\ \cos^2\theta - 1) + \frac{P_{rh}}{r^3}\sin^2\ \theta\cos 2\varphi, \quad (1)$$

where P_{ax} and P_{rh} are the axial and rhombic components of the PAS tensor, respectively, r is the distance between the unpaired electron and the observed nucleus, θ and ϕ are the polar angles describing the orientation of the electron-nucleus vector in the PAS tensor frame. PCS restraints resemble homonuclear dipolar coupling restraints that have been successfully incorporated into XPLOR protocols and used for protein structure refinement (Tjandra et al., 2000). In contrast to homonuclear dipolar couplings, the sign of PCSs is always known. This property significantly simplifies the penalty function that is minimized during simulated annealing refinement:

$$E_{PCS} = k_{PCS}(\Delta\delta_{pc_{calc}} - \Delta\delta_{pc_{obs}})^2, \quad (2)$$

where k_{PCS} is the force constant, and $\Delta\delta_{pc_{calc}}$ and $\Delta\delta_{pc_{obs}}$ are the calculated and observed PCSs. It is straightforward to combine PCSs with NOE restraints in structural refinements using XPLOR-NIH (Schwieters et al., 2003). The PCS restraints were defined using a harmonic potential, similar to residual dipolar couplings, and the restraint describes the

relative position of the paramagnet and the methyl group, where the methyl group position is represented by a pseudoatom, following normal XPLOR protocols. A fully extended starting conformation was used on which 24 000 steps of simulated annealing at 1200 K followed by 15 000 cooling steps of 0.005 ps to 100 K were carried out. Structures (100) were calculated using 356 unambiguous NOE restraints. During the refinement procedure, the distances between the Co^{2+} position and nuclei exhibiting PCSs and the angle between the principal axis of the PAS tensor and the Co^{2+}-nuclear vector were both allowed to vary. The distance between the metal ion and the origin of the PAS frame was fixed. The value of the axially symmetric PAS tensor ($P_{ax} = 870\,000$ ppb Å^3) was determined to be the same for all attachment sites, using the method reported previously (Gaponenko et al., 2002), as was expected, since the ligand field at the Co^{2+} is equivalent for all attachment sites. Non-equivalent PAS tensors would imply differential dynamics, but this was not observed. We observe that only the orientation of the tensor with respect to the molecular frame is different for the three sites. Each set of PCS restraints, corresponding to different attachment sites, was refined against a uniquely defined PAS tensor, and all three tensors were simultaneously included in the structural refinement. This protocol is equivalent to refinement using RDCs from multiple alignment media (Goto et al., 2001). The force constants used for NOE and PCS-derived restraints were 30 kcal mol^{-1} Å^{-2} and 20×10^{-6} kcal mol^{-1} ppb^{-2}, respectively. The PCS force constant was selected by iterative reduction to enable satisfaction of restraints while maintaining good local geometry. The lower and upper bounds for PCS restraints were set to ±20 ppb based on spectral resolution.

Results

In order to provide paramagnetic probe attachment sites, $STAT4_{NT}$ was serially modified at three different positions using S-(2-pyridylthio)-cysteaminyl-EDTA (Toronto Research Chemicals, Inc.). The first position chosen for conjugation was the natively occurring C107. Two other positions, K92 and T50, were selected based on a preliminary, NOE-derived $STAT4_{NT}$ structure, which indicated that these were surface residues lying outside of the dimer interface. For each site, a double mutation was performed to provide a unique EDTA-ligation site. The two mutant proteins contained a C107I substitution, based on homologous STAT proteins. For simplicity, the K92C/C107I and T50C/C107I proteins will be referred to as K92C and T50C. The wild-type and mutant ILV-labeled, ^{2}H, ^{13}C and ^{15}N enriched proteins were prepared according to published procedures (Goto et al., 1999; Zwahlen et al., 1998). The ^{1}H-^{15}N HSQC spectra of the mutants showed only minor chemical shift perturbations in the vicinity of the mutation.

A cobalt (Co^{2+}) paramagnetic probe was bound to EDTA conjugated to the wild type and mutant $STAT4_{NT}$ proteins. Co^{2+} binding to EDTA is tight and specific; however, it should be noted that any non-specific binding to the protein could be mitigated by increasing the ionic strength of the sample. Cobalt was selected because its short longitudinal electronic relaxation time ($\sim 10^{-13}$ s) does not cause significant line-broadening and, therefore, does not degrade the sensitivity or resolution of the NMR spectra. A sub-stoichiometric amount of cobalt was bound in order to populate only one chelation site within the dimer. This condition is important for the determination of the dimer interface (Gaponenko et al., 2002), but is unnecessary in studies of a single polypeptide chain protein. For monomeric proteins we recommend complete saturation with Co^{2+}. Under these conditions, two spectra would be required (Co^{2+}-free and Co^{2+}-saturated) to measure the PCSs, similar to the measurement of RDCs using unaligned and aligned conditions.

Analysis of a ^{13}C CT-HSQC spectrum acquired on a sample of Co^{2+}-bound ILV-labeled ^{15}N, ^{13}C and ^{2}H enriched $STAT4_{NT}$ (Figure 1) illustrates that PCSs for methyl protons can be readily observed. This spectrum exhibits two PCS signals per methyl group, one for each of the two monomeric components of $STAT4_{NT}$. The PCSs can be measured as chemical shift differences between the diamagnetic species and the paramagnetic species. The magnitude of the observed PCSs varied from 20 ppb to 260 ppb. In this example, we will evaluate their utility as structural constraints considering only the set corresponding to one monomer.

A total of 192 ^{1}H PCSs, including 51 PCSs for methyl protons, 127 for H^N protons, and 14 for NH side-chains were measured in the $STAT4_{NT}$ monomer from the three different Co^{2+} attachment sites, using ^{13}C-CT-HSQC, ^{15}N-HSQC and HNCO experiments. Methyl PCSs were only measured for the wt-C107 attachment site, since this was the only species prepared with ILV-methyl protonation. Different positions of

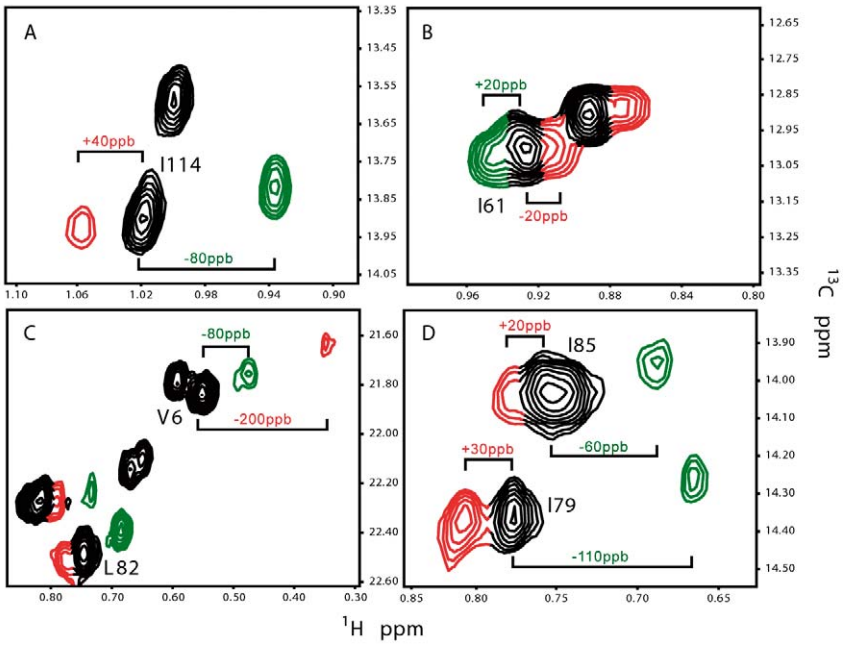

Figure 1. Examples of CH_3 PCSs observed in a ^{13}C CT-HSQC experiment. The data was acquired at 900 MHz with 16 transients and 128 increments in the indirect dimension. The 0.8 mM ILV-labeled ^{2}H, ^{13}C, ^{15}N wt-$STAT4_{NT}$ was dissolved in 10% D_2O 20 mM sodium acetate-d3 (pH 5.3) buffer containing 50 mM NaCl and 0.3 mM $CoCl_2$. Three crosspeaks are observed for each assigned resonance: black is the diamagnetic Co^{2+}-free species, red corresponds to one monomer within the dimer, and green corresponds to the other monomer.

the paramagnetic probe provided different numbers of PCSs. For example, there are only 18 and 11 H^N PCSs for K92C and T50C, respectively. Unobserved PCSs can be explained by unfavorable angles (θ close to 54.7°) and distances from nuclei to the metal ion. In most cases, very long electron-H^N distances (>40 Å) result in significantly reduced PCSs, while short distances (<12 Å) result in line broadening of H^N resonances, due to Curie relaxation effects (Gochin, 1998). We have confirmed the absence of PCSs due to the angular and long distance effects by back calculation following determination of the PAS (*vide infra*).

Discussion

In order to evaluate the impact of PCS restraints on the precision and accuracy of structure determination, two sets of simulated annealing structures were calculated. The first set was calculated using only NOE restraints and the second set included both NOE and PCS restraints. Apart from the inclusion of PCS terms, both calculations were carried out in exactly the same manner. The experimental restraint data included 346 NOEs (2.8 NOEs per residue), 95 TALOS-derived dihedral restraints (Cornilescu et al., 1999), and 192 PCSs (1.6 per residue). The NOEs were comprised of 85 CH_3-CH_3 long range NOEs, 72 H^N-CH_3 long-range NOEs, and 189 H^N-H^N NOEs (mostly short-medium range). H^N-H^N and H^N-CH_3 NOEs were classified into traditional strong, medium and weak categories and converted to distance restraints. Restraints corresponding to CH_3-CH_3 NOEs were defined with loose upper bounds of <7 Å (Gardner et al., 1997). The results of the calculations are summarized in Table 1. When only NOE restraints are used, the backbone RMSD for helical residues from the average structure is 1.4 Å. Introduction of PCS terms only slightly reduces the RMSD to 1.2 Å. The modest improvement in backbone precision by only 0.2 Å provides little insight into the accuracy of the structures.

One assessment of the structural accuracy is provided by a comparison of the solution structures with the crystal structure of the $STAT4_{NT}$ monomer (Vinkemeier et al., 1998) (Figure 2). The pairwise backbone RMSD values for the helical residues between the crystal structure and the solution structures are 2.9 Å for the NOE-based structure and 2.0 Å for the combined NOE and PCS-derived structure. The accuracy of the NOE-based structure is consistent with

Table 1. Summary of restraints and structural statistics

NOE restraints	NOE only structure	PCS + NOE structure
Intraresidue	44	44
Sequential	111	111
Medium range ($i < 5$)	132	132
Long range	59	59
Total NOEs	346	346
ϕ, ψ	95×2	95×2
H-bond[a]	62×2	62×2
PCS restraints		
Wt		98 (H^N)
		14 (NH_2)
		51 (methyls)
K92C		18 (H^N)
T50C		11 (H^N)
Total PCS restraints		192
Total restraints	660	852
Deviations from experimental	$\langle SA \rangle$[b]	$\langle SA \rangle$[b]
RMSD for NOEs	0.0067 ± 0.0020	0.0067 ± 0.0017
NOE violations (>0.3 Å	0	0
ϕ, ψ violations $> 5°$	0	0
PCS violations >40 ppb		0
Deviations from ideal geometry		
Bonds	0.00136 ± 0.0002	0.00137 ± 0.0001
Angles	0.292 ± 0.012	0.293 ± 0.013
Improper	0.138 ± 0.015	0.142 ± 0.017
Precision		
RMSD[c] for ordered backbone atoms, Å	1.4 ± 0.2	1.2 ± 0.2
Accuracy		
RMSD[d] to the crystal structure, Å	2.9	2.0
Q-factor[e]	0.60	0.19
Structure quality		
Procheck (mf/aa/ga/da)[f]	87/12.2/0/0.9	90.4/8.7/0/0.9
XPLOR total energy	71.29 ± 8.81	86.45 ± 14.46

[a]Restraint defined as 1.5 Å between $H^N i$ and O_{i-3} and 2.5 Å between N_i and O_{i-3}.
[b]Average values over the ensemble of 25 lowest energy structures.
[c]Calculated from a superimposition using the backbone atoms of residues 3–8, 12–18, 27–72, 76–95, 97–118.
[d]RMSD between the backbone atoms of residues 3–8, 12–18, 27–72, 76–95, 97–118 compared to the crystal structure of $STAT4_{NT}$ (Vinkemeier et al., 1998).
[e]Q-factors calculated from RDCs that were not used in the structure calculation.
[f]Ramachandran analysis by Procheck (Laskowski et al., 1996): mf = most favored, aa = additionally allowed, ga = generously allowed, da = disallowed.

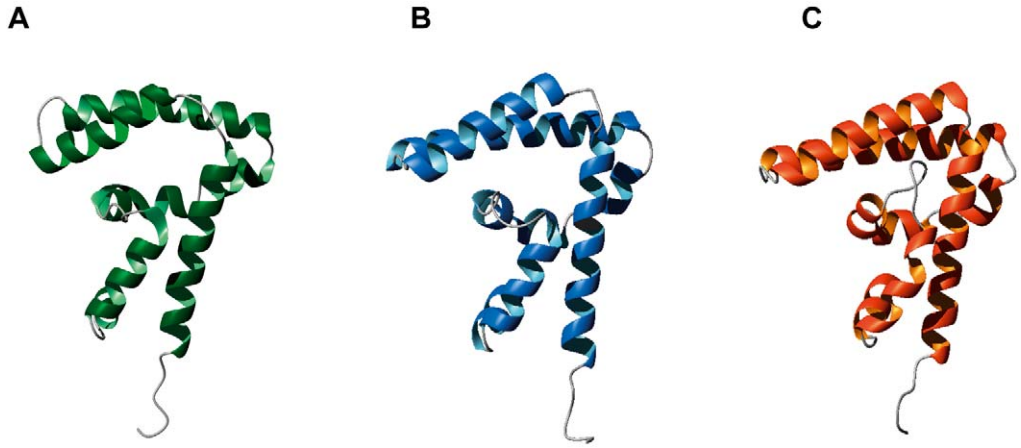

Figure 2. Comparison of the overall topologies of the $STAT4_{NT}$ monomer structure. (A) The solution structure based only on NOEs measurable in ILV-labeled samples (green), (B) the solution structure based on joint refinement with NOE and PCS restraints (blue), and (C) the crystal structure of $STAT4_{NT}$ (orange).

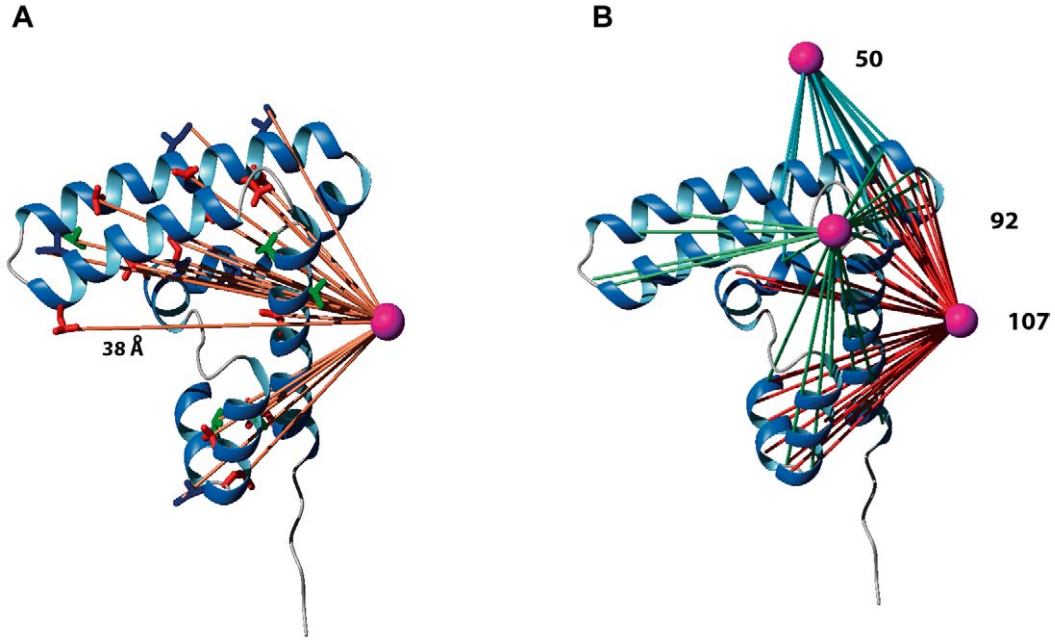

Figure 3. The distribution of measurable PCSs in ILV- $STAT4_{NT}$. Vectors represent the corresponding Co^{2+} to proton distances for (A) methyl groups in Ile, Leu and Val (sidechains shown in green, blue and red, respectively), and (B) amide protons from three different paramagnetic probe attachment sites: C107, T50C, and K92C, as indicated by residue numbers on the right. In (A), the distance (38 Å) corresponding to one Co^{2+}-methyl vector is indicated as an example of the distance range corresponding to measured PCSs.

the predicted RMSD values for ILV-labeled proteins, which range from 2.56 Å to 7.54 Å (Gardner et al., 1997). The 0.9 Å reduction in backbone RMSD is comparable to the result achieved for maltose binding protein (MBP), when RDCs were combined with NOE restraints (Choy et al., 2001). In the MBP calculation, 815 RDCs (2.4/residue) were used to reduce the global backbone RMSD from 4.55 Å to 3.07 Å for MBP, while our results were obtained using only 192 PCS restraints, or 1.5/residue. Since the CH_3 PCS restraints define the position of the terminal methyl groups of I, L and V residues, it is noteworthy to examine the accuracy of the sidechain positions. The RMSD for all heavy atoms of the I, L and V sidechains relative to the crystal monomer structure is 2.97 ± 0.28 Å for the structure ensemble calculated

only with NOE restraints. This value compares favorably to the predicted accuracy for I, L and V sidechains of 2.33 ± 0.92 Å (Gardner et al., 1997). The sidechain RMSD value reduces significantly to 2.43 ± 0.16 Å with the inclusion of PCS restraints. Furthermore, the precision within the ensemble improves from 2.37 ± 0.36 Å for the structure based only on NOE restraints to 1.66 ± 0.26 Å with the inclusion of PCS restraints. Our results show that it is possible to significantly improve both the precision and accuracy obtainable with ILV-labeled proteins when PCS restraints are combined with NOE restraints, and that this improvement can be achieved using fewer restraints.

An independent means to assess the accuracy of an NMR structure is the Q-factor, which is determined from a set of structural data, RDCs, PCSs, or chemical shift anisotropies, not used in the refinement procedure (Ottiger and Bax, 1999). For the wt-$STAT4_{NT}$ monomer, 48 H^N-N RDCs were measured (Gaponenko et al., 2002). The observed RDCs were used to calculate Q for each set of solution structures, and the results are listed in Table 1. Inclusion of PCS restraints significantly improves the quality of calculated structures. This is demonstrated by the reduction of the Q-factor from 0.60 in the case of the NOE-derived structure to 0.19 for the combined NOE and PCS-derived structure. A value of $Q \leq 0.2$ is considered a high-quality solution structure. The basis for the improvement in the $STAT4_{NT}$ structure is illustrated by the distribution of PCS restraints from the three different attachment sites, shown in Figure 3. The long-range (12–40 Å) nature of PCS restraints (supplemental information), distributed across the entire protein structure, enables a much more accurate positioning of secondary structure elements. In contrast, the short-range nature of NOE contacts combined with the paucity of contacts in large perdeuterated proteins, even if ILV-protonated, limits the accuracy of NOE-only structures. A greater number of RDCs are needed to achieve a comparable improvement in the accuracy of the structure, and not all systems may be amenable to the appropriate physical alignment media or exhibit sufficiently high quality spectra to yield the requisite number of RDCs.

Conclusion

It has been demonstrated that PCS and RDC restraints can be readily obtained for non-metallo proteins, *via* designed introduction of paramagnet binding sites, and utilized for structure calculations of large ($\geq$30 kDa), deuterated proteins. When used to augment the ILV-labeling approach to structure determination, PCS restraints provide an improvement in structural accuracy similar to that observed upon addition of a large number of RDC restraints, and this has been demonstrated in the structure determination of the dimerization domain of $STAT4_{NT}$. The improvement in accuracy is cross-validated by Q-factors determined from RDCs measured as a result of magnetic susceptibility alignment. The improvement can be achieved for systems where strong interactions of the protein of interest occurs with known alignment media, precluding the steric alignment and the ability to obtain RDCs. The ability to obtain corroborating data from alternative orientations of the PAS tensor significantly strengthens the value of this long-range structural information. The measurement of PCSs for amide and methyl protons is simple and well suited for generation of structural restraints in very large, highly deuterated systems, where TROSY methods provide resolved H^N-N spectra and rapid internal motions yield resolved H^{methyl}-C COSY spectra.

The assigned chemical shifts for the protein $STAT4_{NT}$ domain, dimer, have been deposited in the BioMagResBank, accession number 5997.

Supplemental material

A table containing the observed PCS values and the associated structural parameters is available from the authors by request.

Acknowledgement

The authors are greatful to Dr Eriks Kupce, Varian, Inc. for use of the 900 MHz spectrometer for part of the data collection.

References

Allegrozzi, M., Bertini, I., Janik, M.B.L., Lee, Y.M., Liu, G. and Luchinat, C. (2000) *J. Am. Chem. Soc.*, **122**, 4154–4161.

Bertini, I., Luchinat, C. and Piccioli, M. (2001) *Meth. Enzymol.*, **339**, 314–340.

Choy, W.Y., Tollinger, M., Mueller, G.A. and Kay, L.E. (2001) *J. Biomol. NMR*, **21**, 31–40.

Cornilescu, G., Delaglio, F. and Bax, A. (1999) *J. Biomol. NMR*, **13**, 289–302.

Delaglio, F., Grzesiek, S., Vuister, G.W., Zhu, G., Pfeifer, J. and Bax, A. (1995) *J. Biomol. NMR*, **6**, 277–293.
Dvoretsky, A., Gaponenko, V. and Rosevear, P.R. (2002) *FEBS Lett.*, **528**, 189–192.
Feeney, J., Birdsall, B., Bradbury, A., Biekofsky, R.R. and Bayley, P.M. (2001) *J. Biomol. NMR*, **21**, 41–48.
Gaponenko, V., Altieri, A.S., Li, J. and Byrd, R.A. (2002) *J. Biomol. NMR*, **24**, 143–148.
Gaponenko, V., Dvoretsky, A., Walsby, C., Hoffman, B.M. and Rosevear, P.R. (2000) *Biochemistry*, **39**, 15217–15224.
Gardner, K.H., Konrat, R., Rosen, M.K. and Kay, L.E. (1996) *J. Biomol. NMR*, **8**, 351–356.
Gardner, K.H., Rosen, M.K. and Kay, L.E. (1997) *Biochemistry*, **36**, 1389–1401.
Gochin, M. (1998) *J. Biomol. NMR*, **12**, 243–257.
Goto, N.K., Gardner, K.H., Mueller, G.A., Willis, R.C. and Kay, L.E. (1999) *J. Biomol. NMR*, **13**, 369–374.
Goto, N.K., Skrynnikov, N.R., Dahlquist, F.W. and Kay, L.E. (2001) *J. Mol. Biol.*, **308**, 745–764.
Grzesiek, S., Vuister, G.W. and Bax, A. (1993) *J. Biomol NMR*, **3**, 487–493.
Hus, J.C., Marion, D. and Blackledge, M. (2000) *J. Mol. Biol.*, **298**, 927–936.
Hus, J.C., Marion, D. and Blackledge, M. (2001) *J. Am. Chem. Soc.*, **123**, 1541–1542.
Kay, L.E. and Gardner, K.H. (1997) *Curr. Opin. Struct. Biol.*, **7**, 722–731.
Kraulis, J., Clore, G.M., Nilges, M., Jones, T.A., Pettersson, G., Knowles, J. and Gronenborn, A.M. (1989) *Biochemistry*, **28**, 7241–7257.
Kraulis, P.J., Domaille, P.J., Campbell-Burk, S.L., Van Aken, T. and Laue, E.D. (1994) *Biochemistry*, **33**, 3515–3531.
La Mar, G.N., Overkamp, M., Sick, H. and Gersonde, K. (1978) *Biochemistry*, **17**, 325–361.
Laskowski, R.A., Rullmannn, J.A., MacArthur, M.W., Kaptein, R. and Thornton, J.M. (1996) *J. Biomol. NMR*, **8**, 477–486.
Montelione, G.T., Emerson, S.D. and Lyons, B.A. (1992) *Biopolymers*, **32**, 327-334.
Mueller, G.A., Choy, W.Y., Yang, D., Forman-Kay, J.D., Venters, R.A. and Kay, L.E. (2000) *J. Mol. Biol.*, **300**, 197–212.
Ottiger, M. and Bax, A. (1999) *J. Biomol NMR*, **13**, 187–191.
Pervushin, K., Riek, R., Wider, G. and Wüthrich, K. (1997) *Proc. Natl. Acad. Sci. USA*, **94**, 12366–12371.
Ramirez, B.E. and Bax, A. (1998) *J. Am. Chem. Soc.*, **120**, 9106–9107.
Rohl, C.A. and Baker, D. (2002) *J. Am. Chem. Soc.*, **124**, 2723–2729.
Schwieters, C.D., Kuszewski, J.J., Tjandra, N. and Clore, G.M. (2003) *J. Magn. Reson.*, **160**, 66–74.
Tjandra, N. and Bax, A. (1997) *Science*, **278**, 1111–1114.
Tjandra, N., Marquardt, J. and Clore, G.M. (2000) *J. Magn. Reson.*, **142**, 393–396.
Tolman, J.R., Flanagan, J.M., Kennedy, M.A. and Prestegard, J.H. (1995) *Proc. Natl. Acad. Sci. USA*, **92**, 9279–9283.
Tugarinov, V., Muhandiram, R., Ayed, A. and Kay, L.E. (2002) *J. Am. Chem. Soc.*, **124**, 10025–10035.
Venters, R.A., Huang, C.C., Farmer, 2nd, B.T., Trolard, R., Spicer, L.D. and Fierke, C.A. (1995) *J. Biomol. NMR*, **5**, 339–344.
Vinkemeier, U., Moarefi, I., Darnell, Jr. J.E. and Kuriyan, J. (1998) *Science*, **279**, 1048–1052.
Zwahlen, C., Gardner, K.H., Sarma, S.P., Horita, D.A., Byrd, R.A. and Kay, L.E. (1998) *J. Am. Chem. Soc.*, **120**, 7617–7625.